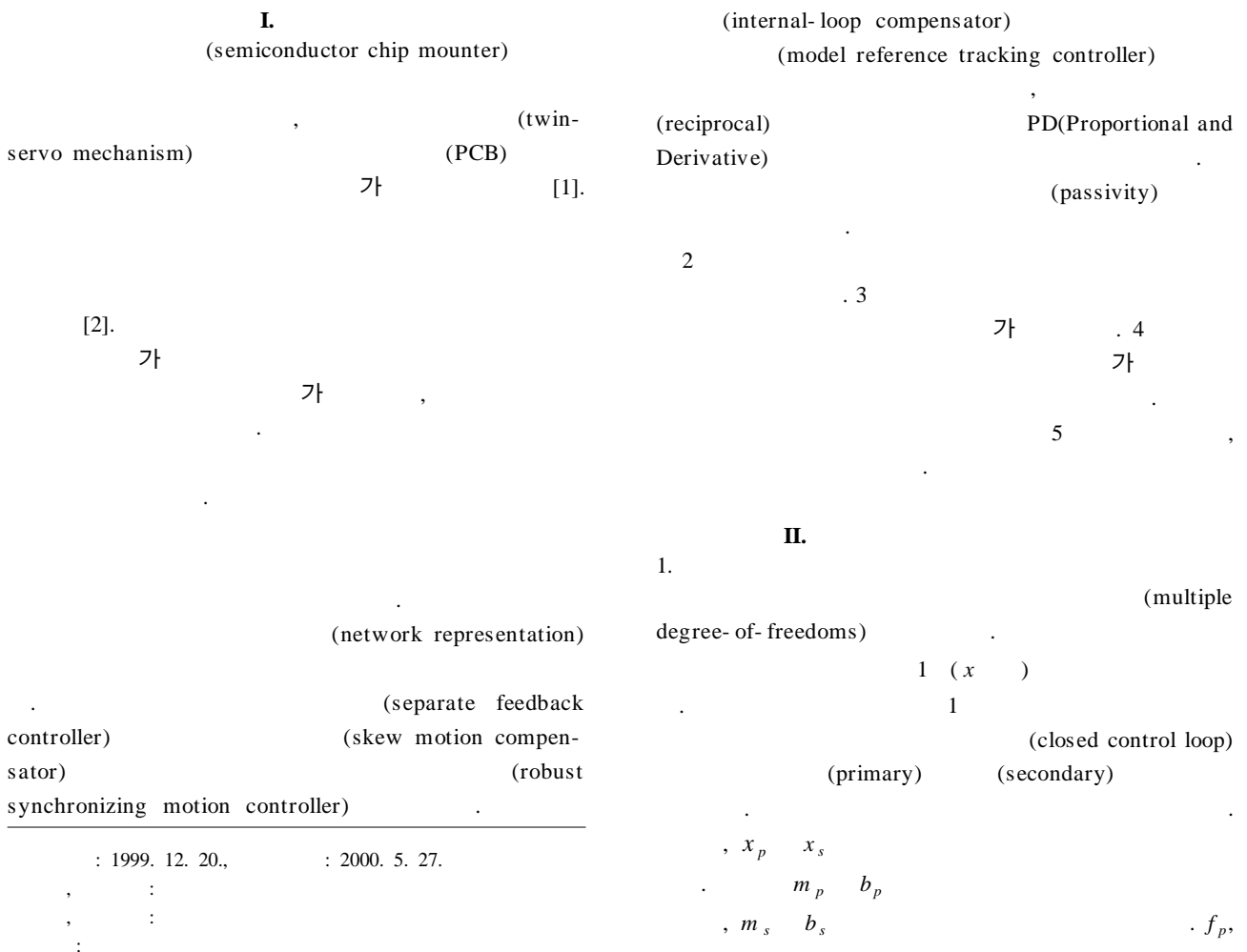


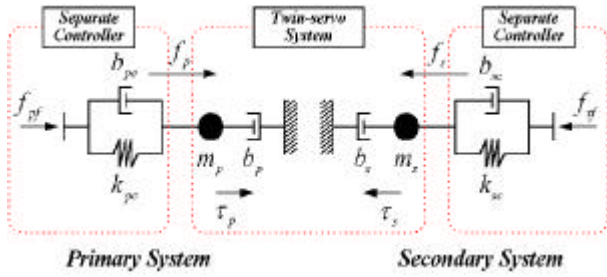
Modeling and Robust Synchronizing Motion Control of Twin-Servo System Using Network Representation

(Bong Keun Kim, Hyun-Taek Choi, Wan Kyun Chung, Il Hong Suh, and Joong Ho Song)

Abstract : A twin-servo mechanism is used to increase the payload capacity and assembling speed of high precision motion control systems such as semiconductor chip mounters. In this paper, we focus on the modeling of the twin-servo system and propose its network representation. And also, we propose a robust synchronizing motion control algorithm to cancel out the skew motion of the twin-servo system caused by different dynamic characteristics of two driving systems and the vibration generated by high accelerating and decelerating motions. The proposed control algorithm consists of separate feedback motion control algorithms for each driving system and a skew motion compensation algorithm. A robust tracking controller based on internal-loop compensation is proposed as a separate motion controller and its disturbance attenuation property is shown. The skew motion compensation algorithm is also designed to maintain the synchronizing motion during high speed operation, and the stability of the whole closed loop system is proved based on passivity theory. Finally, experimental results are shown to illustrate control performance.

Keywords : twin-servo system, network representation, synchronizing motion control, robust internal-loop compensator, passivity





1. Fig. 1. Twin-servo motion control system.

$$\begin{aligned} m_p \ddot{x}_p + b_p \dot{x}_p &= \xi_p + f_p \\ m_s \ddot{x}_s + b_s \dot{x}_s &= \xi_s + f_s \end{aligned} \quad (1)$$

f_s

$$\begin{matrix} \xi_p & \xi_s \\ & 1 \\ & \text{(spring-damper)} \\ & \text{가} \end{matrix}$$

$$\begin{aligned} f_{pf} - f_p &= b_{pc} \dot{x}_p + k_{pc} x_p \\ f_{sf} - f_s &= b_{sc} \dot{x}_s + k_{sc} x_s \end{aligned} \quad (2)$$

b_{pc} k_{pc}

b_{sc} k_{sc}

f_{pf} f_{sf}

(desired trajectory)

(feed-forward)

2.

(skew motion)

가

가

$K_{pp}^{(p,v,a)}$, $K_{ps}^{(p,v,a)}$

(gain)

$K_{sp}^{(p,v,a)}$

$K_{ss}^{(p,v,a)}$ 가

$$\begin{aligned} \xi_p &= \left(K_{pp}^p + K_{pp}^v \frac{d}{dt} + K_{pp}^a \frac{d^2}{dt^2} \right) x_p \\ &\quad - \left(K_{ps}^p + K_{ps}^v \frac{d}{dt} + K_{ps}^a \frac{d^2}{dt^2} \right) x_s \\ \xi_s &= \left(K_{sp}^p + K_{sp}^v \frac{d}{dt} + K_{sp}^a \frac{d^2}{dt^2} \right) x_p \\ &\quad - \left(K_{ss}^p + K_{ss}^v \frac{d}{dt} + K_{ss}^a \frac{d^2}{dt^2} \right) x_s \end{aligned} \quad (3)$$

(3)

(data)

(time delay)

가

(scale)

가

(coupling)

3.

2

(two-terminal-pair)

[3][4].

(impedance)

Z

$$\begin{aligned} V_1 &= z_{11} I_1 + z_{12} I_2 \\ V_2 &= z_{21} I_1 + z_{22} I_2 \end{aligned} \quad (4)$$

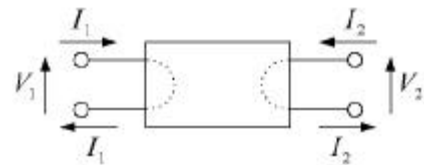
$$Z = \begin{bmatrix} z_{11} & z_{12} \\ z_{21} & z_{22} \end{bmatrix} \quad (5)$$

I_1 I_2

V_1 , V_2

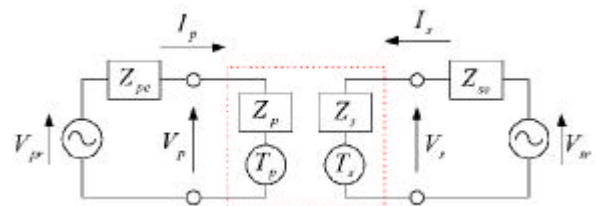
3

(power source)



2.

Fig. 2. Two-terminal-pair network.



3.

Fig. 3. Circuit representation of twin-servo system.

1.

Table 1. Correspondence between mathematical modeling and circuit representation.

| | |
|------------------------|------------------|
| \dot{x}_p, \dot{x}_s | I_p, I_s |
| f_{pr}, f_{sr} | V_{pr}, V_{sr} |
| f_p, f_s | V_p, V_s |
| ξ_p, ξ_s | T_p, T_s |

(1) (3)

$$\begin{aligned} T_p + V_p &= (m_p s + b_p) I_p \equiv Z_p I_p \\ T_s + V_s &= (m_s s + b_s) I_s \equiv Z_s I_s \end{aligned} \quad (6)$$

$$\begin{aligned} T_p &= \left(K_{pp}^a s + K_{pp}^v + K_{pp}^p \frac{1}{s} \right) I_p \\ &\quad - \left(K_{ps}^a s + K_{ps}^v + K_{ps}^p \frac{1}{s} \right) I_s \\ &\equiv P_p I_p - R_p I_s \end{aligned} \quad (7)$$

$$\begin{aligned} T_s &= \left(K_{sp}^a s + K_{sp}^v + K_{sp}^p \frac{1}{s} \right) I_p \\ &\quad - \left(K_{ss}^a s + K_{ss}^v + K_{ss}^p \frac{1}{s} \right) I_s \\ &\equiv P_s I_p - R_s I_s \end{aligned}$$

(6) (7) $T_p \quad T_s$

$$\mathbf{Z} = \begin{bmatrix} Z_p - P_p & R_p \\ -P_s & Z_s + R_s \end{bmatrix} \quad (8)$$

2 I_1, I_2, V_1, V_2 3 I_p, I_s, V_p, V_s $|\mathbf{Z}|$

$$|\mathbf{Z}| = (Z_p - P_p)(Z_s + R_s) + P_s R_p \equiv D \quad (9)$$

$$\begin{aligned} Z_{pc} &= b_{pc} + k_{pc} \frac{1}{s} \\ Z_{sc} &= b_{sc} + k_{sc} \frac{1}{s} \end{aligned} \quad (10)$$

(10) (2)

$$Z_{pc} \quad Z_{sc}$$

(10)

III.

2 가 가

Q

[5][6].

1.

(Single Input Single

Output, SISO)

$$u = u_r + K(y_r - y) \quad (11)$$

y (output) , y_r

, u_r

K (Laplace)

s 4

(11) (Robust Internal-loop

Compensator, RIC)

[6][7].

4

u_r ,

(disturbance) d,

(measurement noise) ξ

(12)

$$y = G_{u,y} u_r + G_{d,y} d + G_{\xi,y} \xi \quad (12)$$

$$G_{u,y} = \frac{P(1 + P_m K)}{1 + PK}$$

$$G_{d,y} = \frac{P}{1 + PK} \quad (13)$$

$$G_{\xi,y} = \frac{PK}{1 + PK}$$

(14)

(model following error)

$$e_r = y_r - y \quad (14)$$

(12) (14)

$$e_r = S \{ (P_m - P) u_r - P d \} + T \xi \quad (15)$$

(sensitivity function) S

(complementary sensitivity function) T

$$S = \frac{1}{1 + PK}, \quad T = \frac{PK}{1 + PK} \quad (16)$$

$$S = 0 \quad T = 0$$

(16)

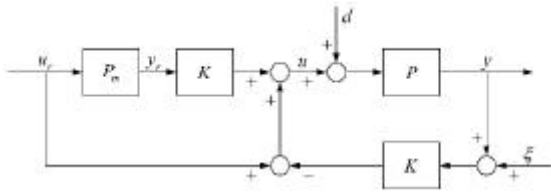
$$S + T = 1$$

가 가 S T H_∞

[6][7].

$$(13) \quad G_{dy} = \frac{K}{P_m}$$

(bandwidth) $G_{dy} \approx 0$



4.

Fig. 4. Robust internal-loop compensator structure.

2. Q

[5][8].

Q (low-pass filter) 가 , Q (cutoff frequency)

가

[9].

Q , Q 가 (explicit function)

가 [10].

Q 가 (implicit function)

Q 가

Q

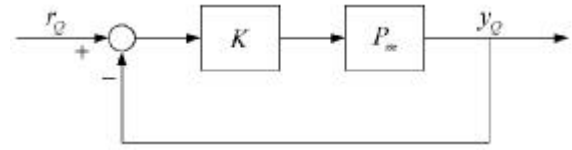
가

K S T 가 가

5 가

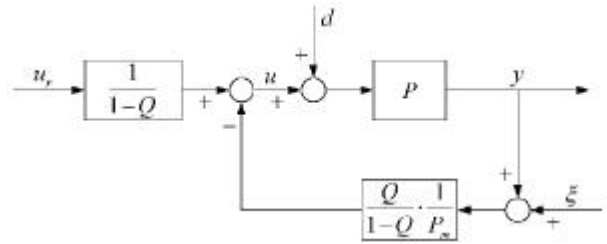
Q Q P_m K

Q



5. Q .

Fig. 5. Transfer function Q .



6. Q

가

Fig. 6. Equivalent structure of RIC using Q .

$$Q = \frac{P_m K}{1 + P_m K} \quad (17)$$

K

$$K = \frac{Q}{P_m(1-Q)} \quad (18)$$

K

4

6

[5].

$$\begin{aligned} G_{u,y} &= \frac{P P_m}{P_m(1-Q) + P Q} \\ G_{dy} &= \frac{P P_m(1-Q)}{P_m(1-Q) + P Q} \\ G_{\xi y} &= - \frac{P Q}{P_m(1-Q) + P Q} \end{aligned} \quad (19)$$

Q

$$Q \approx 1, \quad (19)$$

$$G_{dy} \approx 0$$

가

(multi-variable)

Remark 1.

P_m

K

$$P_m = \frac{1}{m s^2 + b s}, \quad K = \left(K_p + K_i \frac{1}{s} + K_d s \right) \quad (20)$$

(17) Q 가

$$Q = \frac{K_d s^2 + K_p s + K_i}{m s^3 + (b + K_d) s^2 + K_p s + K_i} \quad (21)$$

$$K_p = b g, \quad K_i = 0, \quad K_d = m g$$

$$Q = \frac{g}{s + g} \quad (22)$$

가 , g Q 가
 $K_p = 3\zeta, K_i = 1, K_d = 0, m = \zeta^3, b = 3\zeta^2$
 가 (relative degree)가 2 (bilinear filter) 가

$$Q = \frac{3(\zeta s) + 1}{(\zeta s)^3 + 3(\zeta s)^2 + 3(\zeta s) + 1} \quad (23)$$

Remark 2. Q 가 [5][10].

$$K, \quad (17) \quad Q \quad P_m$$

K [6][7].

3.

$$m \ddot{x} + b \dot{x} = f \quad (24)$$

$$, f \quad (25)$$

$$e = x_d - x \quad (25)$$

, x_d (desired trajectory) (11)

$$f = f_r + K(x_r - x) \quad (26)$$

$$, K, \quad , f_r \quad (27)$$

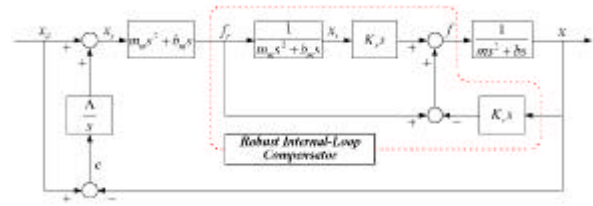
$$f_r = m_m \ddot{x}_r + b_m \dot{x}_r \quad (27)$$

(state)

$$, m_m \quad b_m, \quad , x_r \quad (27)$$

(24) 가

가



7.

Fig. 7. Robust model reference control structure.

$$x_r = x_d + \int_0^t e dt \quad (28)$$

$$, \int \quad (24)$$

(27)

$$x_r - x = e + \int_0^t e dt \quad (29)$$

$$(29) \quad (30)$$

$$\dot{x}_r - \dot{x} = \dot{e} + \int e dt \equiv r, \quad (30)$$

$$f = m_m \ddot{x}_r + b_m \dot{x}_r + K_r r \quad (31)$$

Remark 3. (26) (31) P_m

K

$$P_m = \frac{1}{m_m s^2 + b_m s}, \quad K = K_r s \quad (32)$$

$$(32) \quad (17) \quad Q$$

$$Q = \frac{K_r / m_m}{s + (b_m + K_r) / m_m} \quad (33)$$

$$b_m \quad K_r$$

K_r / m_m Q 가

$$Q \approx 1$$

Remark 4.

$$f_r - f = b_c \dot{x} + k_c x \quad (34)$$

$$\begin{aligned} f_f &= m_m (\ddot{x}_d + \int \dot{x}_d) + (b_m + K_r) (\dot{x}_d + \int x_d) \\ b_c &= m_m \int + K_r \\ k_c &= (b_m + K_r) \int. \end{aligned} \quad (35)$$

$$(2) \quad f_r, \quad , b_c$$

k_c

가

IV.

(reciprocal)

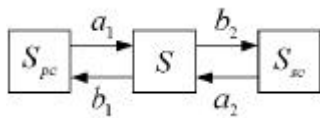
1.

$f_{(p,s)}$,
 $\zeta_{(p,s)}$

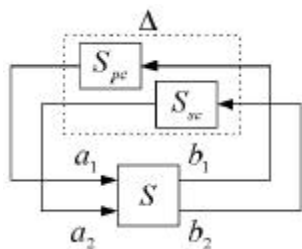
2.

$$b = S a \tag{36}$$

S (scattering matrix) a b
(wave)



(a)



(b)

8.

Fig. 8. Scattering form of the twin-servo system.

$$a = [a_1, a_2]^T \equiv \frac{V + I}{2} \tag{37}$$

$$b = [b_1, b_2]^T \equiv \frac{V - I}{2}$$

$V = [V_p, V_s]^T$, $I = [I_p, I_s]^T$
(power)가

(passive)

$$P = \text{Re}(V_p^* I_p - V_s^* I_s)$$

$$= a^* a - b^* b \tag{38}$$

$$= a^* (E_2 - S^* S) a \geq 0$$

$*$ (conjugate transpose)

E_2 2×2 (identity matrix)

$$\|S\|_\infty = \overline{Q}(S(j\omega))$$

$$= \sup_\omega \sqrt[1/2]{(S(j\omega)^* S(j\omega))} \leq 1 \tag{39}$$

8(a) (scattering

form)

8(b)

(virtual environment)

가 (virtual

$$\mathcal{V} = \begin{bmatrix} S_{pc} & 0 \\ 0 & S_{sc} \end{bmatrix} \tag{40}$$

(35)

(time invariant)

$$|S_{pc}| \leq 1$$

$$|S_{sc}| \leq 1$$

$$\|\mathcal{V}\|_\infty \leq 1$$

[11][12].

1 :

S 가 $\text{Re}(s) \geq 0$

(analytic)

\mathcal{V}

S

(structured singular value)

1

$$\kappa_{\mathcal{V}}(S) \leq 1, \quad \Delta^\infty \tag{41}$$

\mathcal{V} \mathcal{V}

C

$$\mathcal{V} = \{ \text{diag} [\mathcal{V}_1, \mathcal{V}_2] : \mathcal{V}_i \in C \} \tag{42}$$

S 가

$$\kappa_{\mathcal{V}}(S) = \|S\|_\infty \tag{43}$$

S

$$S = \frac{1}{D + z_{11} + z_{22} + 1}$$

$$\times \begin{bmatrix} D + z_{11} - z_{22} - 1 & 2z_{12} \\ 2z_{21} & D - z_{11} + z_{22} - 1 \end{bmatrix} \tag{44}$$

(39)

2.

가

가

PD(Proportional and

Derivative)

$$\begin{aligned} \xi_p &= k_p(x_s - x_p) + k_d(\dot{x}_s - \dot{x}_p) \\ \xi_s &= k_p(x_p - x_s) + k_d(\dot{x}_p - \dot{x}_s) \end{aligned} \quad (45)$$

$$P_m = \begin{bmatrix} k_p & k_d \\ 0 & 0 \end{bmatrix} \quad (33)$$

$$Q = \begin{bmatrix} 1 & 0 \\ 0 & 1 \end{bmatrix} \quad (32)$$

$$S = \begin{bmatrix} \alpha & \beta \\ 0 & 0 \end{bmatrix} \quad (44)$$

$$S = \frac{1}{(1 + \alpha)(1 + \alpha + 2\beta)} \times \begin{bmatrix} \alpha(\alpha + 2\beta) - 1 & -2\beta \\ -2\beta & \alpha(\alpha + 2\beta) - 1 \end{bmatrix} \quad (46)$$

$$\alpha = m_m s + b_m, \quad \beta = \frac{k_p}{s} + k_d \quad (47)$$

$$S = \begin{bmatrix} \alpha_1 & 0 \\ 0 & \alpha_2 \end{bmatrix} \quad (48)$$

$$\begin{aligned} \alpha_1 &= \frac{|\alpha - 1|}{|\alpha + 1|} \leq 1 \\ \alpha_2 &= \frac{|\alpha + 2\beta - 1|}{|\alpha + 2\beta + 1|} \leq 1 \end{aligned} \quad (39)$$

$$f_{pr} \quad f_{sr}$$

V.

9

10

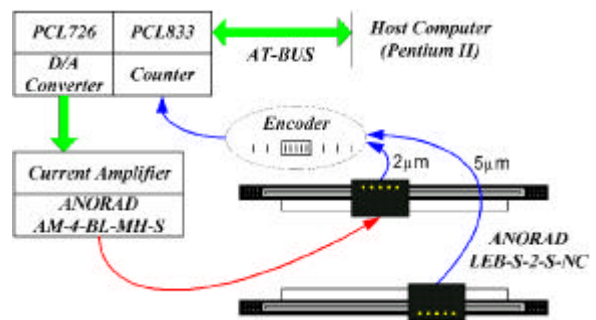
(host computer) 1 msec
 , 12-bit D/A (digital/analogue converter; ADVANTECH, PCL-726)
 , (DC servo amplifier; ANORAD, AM-4-BL-MS-S) (direct drive)
 (lineaar servo motor; ANORAD, LEB-S-2-S-NC) 2µm, 5µm
 가 (RSF Elektronik, MS44)
 (counter card; ADVANTECH, PCL-833)

$$\begin{aligned} 0.55 \ddot{x}_p + 0.4 \dot{x}_p &= \xi_p + f_p \\ 0.45 \ddot{x}_s + 0.3 \dot{x}_s &= \xi_s + f_s \end{aligned} \quad (49)$$



9.

Fig. 9. Twin-servo precision linear motor system.



10.

Fig. 10. Hardware configuration of twin-servo system.

(31)

$$f_{(p,s)} = m_m (\ddot{x}_d + \nabla_d \dot{e} + \nabla_p e) + K e_r \quad (50)$$

$$\nabla_p = 3000, \quad \nabla_d = 100$$

(double integrator)

$$P_m = \frac{1}{0.5s^2} \quad (51)$$

, K H_∞ (mixed sensitivity method) [6][13].

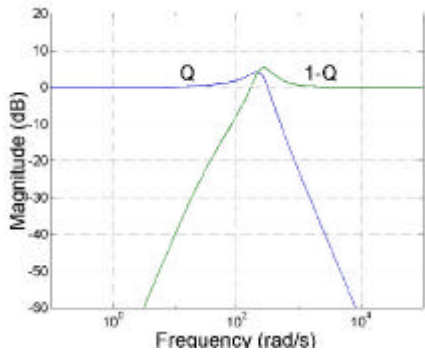
$$K = \frac{(9.4550 \times 10^9)s + (3.0231 \times 10^{11})}{s^2 + (2.7659 \times 10^5)s + (6.0826 \times 10^7)} \quad (52)$$

11 (51) (52) (17) Q

(1- Q) Bode

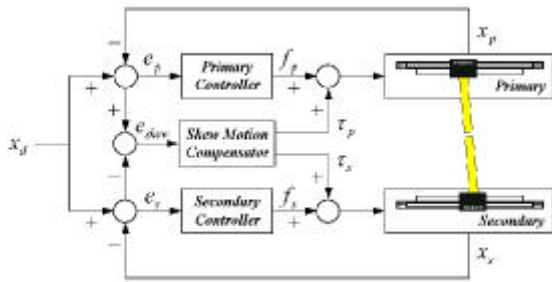
(45) PD

$$\begin{aligned} \xi_p &= k_p e_{skew} + k_d \dot{e}_{skew} \\ \xi_s &= -k_p e_{skew} - k_d \dot{e}_{skew} \end{aligned} \quad (53)$$



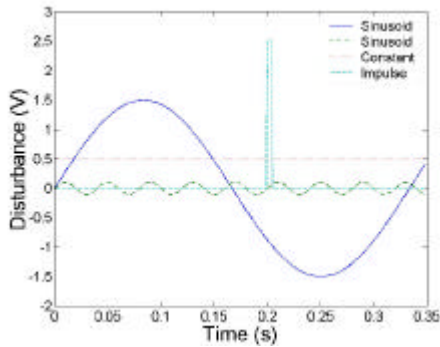
11. Q $(1-Q)$ Bode

Fig. 11. Bode plot of the designed Q and $(1-Q)$.



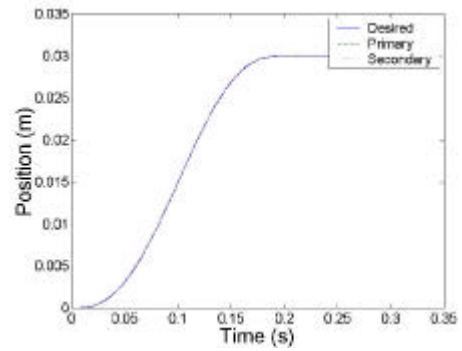
12.

Fig. 12. Robust synchronizing motion control structure.

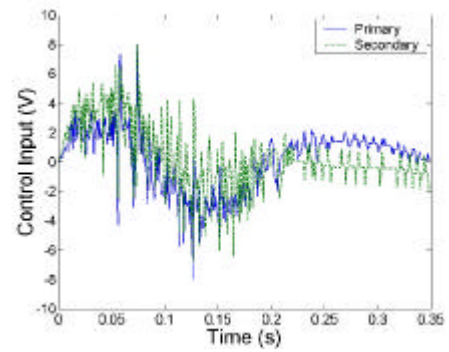


13.

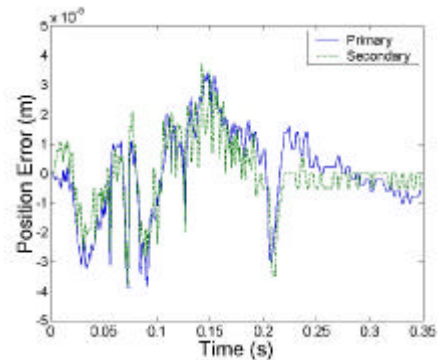
Fig. 13. Disturbance applied to the twin-servo system.



(a)



(b)



(c)

14.

Fig. 14. Experimental results with disturbance.

$e_{skew} = x_s - x_p$, K_p
 $50, K_d = 15$
 12
 5
 30 mm
 (discretization)

14 13
 $\mp 40 \mu\text{m}$

VI.

PD

(brush)가 DC

가

[1] B. K. Kim, W. K. Chung, K. B. Lee, J. H. Song, and I. Choy, "Modeling and synchronizing motion control of twin-servo system," *Proc. 1999 Korea Automatic Control Conference*, pp. 302-305, 1999.

[2] , , , "2 ,," 1998 , pp. 436-439, 1998.

[3] G. J. Raju, G. C. Verghese, and T. B. Sheridan, "Design issues in 2-port network models of bilateral remote manipulation," *Proc. 1989 IEEE Int. Conf. on Robotics and Automation*, pp. 1316-1321, 1999.

[4] Y. Yokokohji and T. Yoshikawa, "Bilateral control of master-slave manipulators for ideal kinesthetic coupling-formulation and experiment," *IEEE Trans. on Robotics and Automation*, vol. 10, no. 5, pp. 605-620, October, 1994.

[5] H. S. Lee and M. Tomizuka, "Robust motion controller design for high-accuracy positioning systems," *IEEE Trans. on Industrial Electronics*, vol. 43, no. 1, pp. 48-55, February, 1996.

[6] B. K. Kim, W. K. Chung, H. T. Choi, I. H. Suh, and

Y. H. Chang, "Robust optimal internal loop compensator design for motion control of precision linear motor," *Proc. 1999 IEEE Int. Symposium on Industrial Electronics*, pp. 1045-1050, 1999.

[7] B. K. Kim, W. K. Chung, H. T. Choi, I. H. Suh, H. S. Lee, and Y. H. Chang, "Robust time optimal controller design for HDD," *IEEE Trans. on Magnetics*, vol. 35, no. 5, pp. 3598-3600, 1999.

[8] H. T. Choi, B. K. Kim, I. H. Suh, and W. K. Chung, "Design of robust high-speed motion controller with actuator saturation," to be appeared in *Trans. ASME J. of Dyn. Syst., Meas. and Contr.*

[9] B. Yao, M. Al-Majed, and M. Tomizuka, "High performance robust motion control of machine Tools: An adaptive robust control approach and comparative experiments," *IEEE/ASME Trans. on Mechatronics*, vol. 2, no. 2, pp. 63-76, June, 1997.

[10] K. Yamada, S. Komada, M. Ishida, and T. Hori, "Analysis and classical control design of servo system using high order disturbance observer," *Proc. 1998 IEEE Int. Conf. on Industrial Electronics, Control, and Instrumentation*, pp. 4-9, 1998.

[11] J. E. Colgate, "Power and impedance scaling in bilateral manipulation," *Proc. 1991 IEEE Int. Conf. on Robotics and Automation*, pp. 2292-2297, 1991.

[12] T. Yoshikawa and J. Ueda, "Analysis and control of master-slave systems with time delay," *Proc. 1996 IEEE/RSJ Int. Conf. on Intelligent Robots and Systems*, pp. 1366-1373, 1996.

[13] Richard Y. Chiang and Michael G. Safonov, *Robust Control Toolbox*, Mathworks, Inc. 1992.



1994
(1996), 1996



1991
(1993), 1993 1995
1995



1981
(1983),
(1987),
1987



1977
1982
(). 1982
. 1987-1988



1980

(1982),
(1993), 1995- 1996
, 1982- 1985
, 1985 -